J. Physiol. (1982), **323**, *pp.* 287–306
With 11 *text-figures*
Printed in Great Britain

CONDUCTION BLOCK IN RAT MYELINATED FIBRES FOLLOWING ACUTE EXPOSURE TO ANTI-GALACTOCEREBROSIDE SERUM

BY SERGE LAFONTAINE*, MICHAEL RASMINSKY*†, TAKAHIKO SAIDA‡ AND AUSTIN J. SUMNER‡

*From the *Neurosciences Unit, Montreal General Hospital, Department of Neurology and Neurosurgery, McGill University, 1650 Cedar Avenue, Montreal, Quebec H3G 1A4, Canada, and the ‡Department of Neurology, University of Pennsylvania, Philadelphia, PA 19104, U.S.A.*

(*Received 27 March 1981*)

SUMMARY

1. We have observed conduction in single rat spinal ventral root nerve fibres following acute topical application of anti-galactocerebroside serum.

2. Conduction of nerve impulses was initially slowed and subsequently blocked at the site of serum exposure.

3. Conduction block occurred within as little as 1 hr in more slowly conducting (20–30 m/sec) myelinated fibres but occurred later in fibres conducting more rapidly.

4. Conduction block was preceded by a rise in internodal conduction time from the normal 20 μsec to about 200 μsec.

5. At nodes exposed to serum, conduction block was invariably associated with greatly decreased depolarization; this was contrasted with nodes exposed to local anaesthetic or tetrodotoxin where conduction block occurred despite nodal depolarization well beyond threshold potential.

6. Nodal capacitance and resistance were estimated from simultaneous recordings of membrane current and extracellular potential at blocked nodes exposed to local anaesthetic or tetrodotoxin (normal nodes) and at blocked nodes exposed to anti-galactocerebroside serum.

7. For normal fibres of internodal length 0·8–1·1 mm, an upper limit estimate for average nodal capacitance was $2{\cdot}6 \pm 0{\cdot}3$ pF and a lower limit estimate for average nodal resistance was 55 ± 10 MΩ. There was an order of magnitude increase in the capacitance of nodes at which conduction block occurred following exposure to anti-galactocerebroside serum.

8. We conclude that the early conduction block caused by anti-galactocerebroside serum is due to paranodal demyelination and that acute paranodal demyelination is sufficient to cause conduction block.

† To whom reprint requests should be sent.

INTRODUCTION

Intraneural injection of serum from rabbits hyperimmunized with galactocerebroside produces antibody-mediated, complement-dependent conduction block in peripheral nerves. Following micro-injection of anti-galactocerebroside serum (AGS) into rat sciatic nerve, the amplitude of the muscle response elicited by motor nerve stimulation proximal to the injection site begins to fall within 30 min, and conduction block in the majority of motor axons occurs within 3–4 hr without significant fall in maximal conduction velocity (Saida, Sumner, Saida, Brown & Silberberg, 1980; Sumner, 1981; Sumner, Saida, Saida, Silberberg & Asbury, 1981). The morphological changes observed during the 5 hr following serum injection include swelling of Schwann cells, widening of Schmidt–Lanterman clefts and early paranodal demyelination in some axons (Saida, Saida, Brown & Silberberg, 1979).

Two possible mechanisms could be responsible for acute conduction block following exposure to the antiserum: (1) changes in the cable properties of fibres secondary to the minimal morphological changes and (2) changes in the electrical excitability of axon membrane at nodes of Ranvier. In order to examine the mechanism of antibody-mediated conduction block we have observed propagation of nerve impulses in single rat spinal root fibres focally exposed to AGS. We have found that conduction block is indeed associated with substantial changes in the cable properties of fibres exposed to the serum.

METHODS

Experiments were performed on adult (300–450 g) Sprague–Dawley rats.

Preparation of animals for experiments

Anaesthesia was induced with sodium pentobarbitone (50 mg/kg body wt. I.P.) and following tracheostomy a surgical level of anaesthesia was maintained throughout the experiment by inhalation of Fluothane in oxygen. A total lumbar laminectomy was performed and the tail dissected as described by Rasminsky & Sears (1972) to expose the left ventral caudal nerve and its branches to the intersegmental tail muscles. The experimental preparation is illustrated in Fig. 1. The mineral oil pool over the laminectomy site was maintained at 37 °C by a thermostatically regulated heating device in the pool and a mixture of 95 % O_2–5 % CO_2 was bubbled continuously in the pool. The mineral oil pool over the tail was at ambient room temperature.

Single fibres or small groups of fibres were excited by stimulation of muscular branches of the ventral caudal nerve. After conduction antidromically, impulses were recorded from the appropriate sacral or coccygeal ventral root from pairs of wire (Ag or Pt–Ir) electrodes. In most experiments roots were maintained in continuity.

Anti-galactocerebroside serum

The sera used in these experiments were obtained from New Zealand albino rabbits hyperimmunized with galactocerebroside (Saida *et al.* 1979). These sera had previously been shown to have strong *in vivo* electrophysiological blocking activity in the sciatic nerve preparation (Sumner, 1981; Sumner *et al.* 1981). This blocking activity was lost after heating to 56 °C for 30 min and was restored by the addition of fresh complement. It was also removed by prior absorption by purified C.N.S. or P.N.S. myelin or by purified galactocerebroside but not by glucocerebroside or liver. Sera were stored at −70 to −90 °C and were thawed immediately prior to application to the spinal roots.

Topical application of AGS

A ventral root containing units responding to peripheral stimulation was gently lifted over a small well about 4 mm long, 2 mm wide and 1 mm deep. The ends of the well were coated with petroleum jelly and care was taken to minimize traction on the root as it rested on the well. With a 0·5 ml.

syringe and a fine gauge (no. 30) needle a drop of serum was injected into the well under direct visualization through a dissecting microscope and could be seen to envelop the root over the length of about 4 mm defined by the ends of the well. This drop of serum could be observed to remain in the same position on the root for many hours as the experiment progressed.

Recording techniques

Latency measurements. In the initial experiments two pairs of recording electrodes were placed 11·5–16 mm apart, one on the proximal and one on the distal side of the well (Fig. 1) and the latency of conduction in single fibres across the well was repeatedly determined before and after application of the serum. The distance between the recording electrodes was measured with a pair of calipers

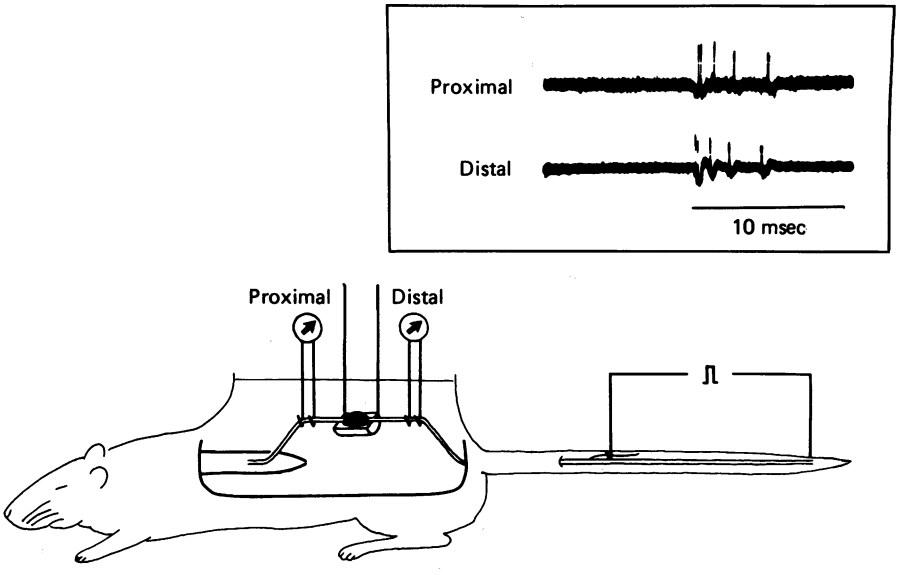

Fig. 1. Schematic diagram of the experimental preparation. The inset shows responses in five single fibres recorded at sites distal and proximal to the well containing AGS.

and conduction velocity prior to serum application determined for each unit. The recording electrodes were 125 μm Ag wires separated by about 600 μm, led to the inputs of differential amplifiers with input impedance 10^8 Ω (Neurolog 100, Digitimer Ltd.). After further amplication responses were recorded on magnetic tape using direct channels of a Racal Store 4 tape recorder with low-frequency cut-off at 100 Hz, the high frequency response of the recording system being limited to 10 kHz.

Internodal conduction. Propagation of impulses along the ventral roots was observed by recording external longitudinal current at intervals along the root (Rasminsky & Sears, 1972) from a pair of 125 μm Ag wires separated by about 350 μm. These scanning electrodes were led to the inputs of a differential amplifier (Neurolog 100, Digitimer Ltd.) with high frequency response set to > 35 kHz. Recordings were also made differentially from a more distal pair of immobile 125 μm Ag electrodes separated by about 600 μm so that spike-triggered averaging of potentials from single fibres could be carried out (Bostock & Sears, 1978). The high-frequency response for recording from these reference electrodes was set to 10 kHz. These experiments were recorded on magnetic tape (band pass 100 Hz–19 kHz) and subsequently played back into a Nicolet 1070 averaging computer for A/D conversion. Data were then transferred to the memory of a PDP 11/34 computer and stored on disk for subsequent analysis.

In these experiments single fibres were usually stimulated at 10 Hz and thirty-two to sixty-four responses were averaged at each recording site. Although no current calibration was used for the external longitudinal current records, and although any low-frequency (< 100 Hz) component of

the signals would have been distorted by the tape recorder, the sites of local maxima of external longitudinal current were easily recognized (Fig. 6) and internodal conduction times were determined as the latency between successive maxima.

Membrane current and membrane potential. In some experiments the ventral roots were cut at the spinal cord and external longitudinal currents were recorded between a pair of 25 μm Pt–Ir electrodes separated by 150 μm (Fig. 2). The more proximal of the two Pt–Ir electrodes was also used to record potential with respect to a third electrode on the killed end of the root. Spike-triggered averaging from a distal pair of recording electrodes was used for these unit recordings, 128–512 iterations usually being averaged on-line by the Nicolet 1070 computer at a digitization rate of 5 or 10 μsec per bin, the band pass of the recording system being 10 Hz to > 35 kHz.

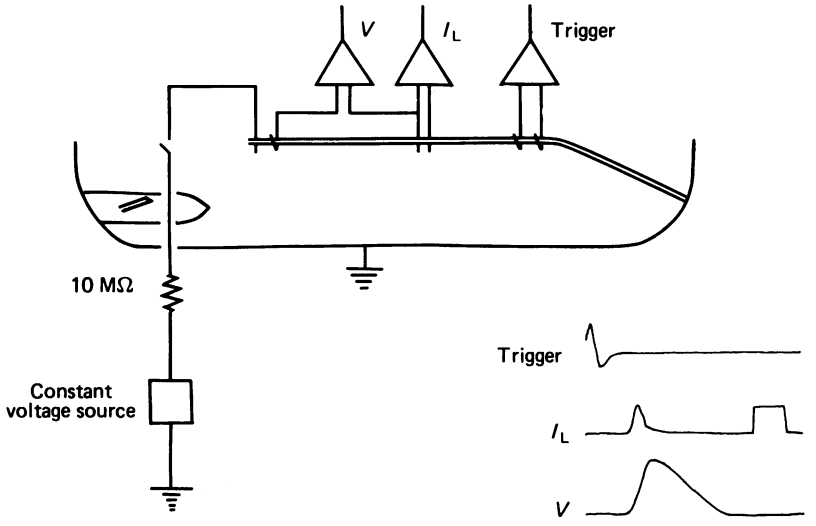

Fig. 2. Schematic diagram of the experimental preparation for recordings of external longitudinal current and extracellular potential. The impulse recorded at the distal electrodes triggers the averager for recordings at the more proximal electrodes and also triggers, with a delay, the calibration signal from the constant voltage source.

For the external longitudinal current recordings, a constant-voltage source in series with a 10 MΩ resistor delivered a constant-current calibration pulse which passed from the killed end of the root to ground, the calibration pulse being triggered with an appropriate delay by the spike recorded at the distal electrodes. The averaged external longitudinal current recordings were subsequently normalized by the computer with reference to the calibration current. Membrane currents at successive sites along the root were then derived by differencing adjacent external longitudinal current records (Rasminsky & Sears, 1972; Bostock & Sears, 1978).

Alternate measurements of external longitudinal current and potential were made at each recording site and the scanning electrodes were then moved to the next site. The active electrode for the potential recordings was the more proximal of the two mobile electrodes. As the separation between the two scanning electrodes was about 150 μm and the excursion between recordings 200 μm, the potential recordings were made from a point on the nerve within about 25 μm of the mid point of the length of the fibre over which average membrane current was determined.

The change in extracellular monophasic action potential ΔV_o is related to the transmembrane potential change ΔV_m by the equation

$$\frac{\Delta V_o}{\Delta V_m} = \frac{-r_o}{r_o + r_i},$$

where r_o and r_i are the extracellular and intracellular resistances respectively (Katz, 1966). For the calculations of membrane capacitance and resistance outlined below, we have assumed that the ratio of r_o and r_i remained fixed along the length of the fibre and that the amplitude of the action potential in the normal portion of the recorded fibres was 100 mV (Brismar, 1980). We have scaled the extracellularly recorded potentials accordingly.

Estimation of nodal capacitance and resistance

For a patch of nerve membrane, the membrane current i_m is divided into resistive and capacitive components such that

$$i_m = \frac{1}{r_m}\Delta V_m(t) + c_m \frac{d}{dt}\Delta V_m(t), \tag{1}$$

where r_m is membrane resistance in ohm-cm, c_m is membrane capacitance in farads-cm^{-1} and ΔV_m is the displacement of the membrane potential V_m from its resting value. If a node of Ranvier is included within the length of fibre over which membrane current is measured, the membrane current will comprise principally current flowing through the node i_n and eqn. (1) is approximated by

$$i_n = \frac{1}{r_n}\Delta V_m(t) + c_n \frac{d}{dt}\Delta V_m(t), \tag{2}$$

where r_n is nodal resistance in ohms and c_n is nodal capacitance in farads. If $i_n(t)$ and $\Delta V_m(t)$ are known, eqn. (2) can then in principle be solved for r_n and c_n providing that these quantities are not time or voltage dependent.

Equation (2) can be rewritten in the discrete time form (Smith, 1977):

$$\Delta V_k = e^{-T_s/\tau_m}\Delta V_{k-1} + r_n(1-e^{-T_s/\tau_m})\, i_k, \tag{3}$$

where T_s is the sampling period, ΔV_k is the displacement of membrane potential from resting potential at the kth sampling time, i_k is the nodal current at the kth sampling time and τ_m is the nodal membrane time constant equal to $r_n c_n$.

Equation (3) can be rewritten as

$$\Delta V_k = a_0 \Delta V_{k-1} + b_0 i_k, \tag{4}$$

where

$$a_0 = e^{-T_s/\tau_m}, \tag{5}$$

and

$$b_0 = r_n(1-e^{T_s/\tau_m}). \tag{6}$$

The experimentally obtained records of potential and membrane current were sampled over most or all of the time domain of the nodal action potential; values for a_0 and b_0 were estimated by direct minimization of the mean-square error between the model output and the experimental data (Rosenbrock, 1966). From the estimates of a_0 and b_0, values for r_n and c_n were then obtained by solving eqns. (5) and (6) to give:

$$r_n = \frac{b_0}{1-a_0}, \tag{7}$$

$$c_n = \frac{-T_s(1-a_0)}{b_0 \ln a_0}. \tag{8}$$

The foregoing computations were performed on a PDP 11/34 computer.

RESULTS

Development of conduction block after exposure to AGS

Fig. 3 illustrates for a single fibre the change in latency across the short length of root containing the site of immersion in AGS. In this unit the change in latency is relatively small during the first hour following serum application but latency increases rapidly over the next hour until conduction block ensues after 120 min.

The latency across the well for this fibre and for the four other simultaneously

recorded fibres is shown in Fig. 4 as a function of time before and after serum application. Latency remains constant for each fibre during the control period. Following serum application the latency begins to increase first in the more slowly conducting, smaller diameter fibres and subsequently in the more rapidly conducting, larger diameter fibres. Conduction block occurs earlier in the more slowly conducting fibres. An increase in latency of several hundred μsec was invariably seen before conduction block occurred.

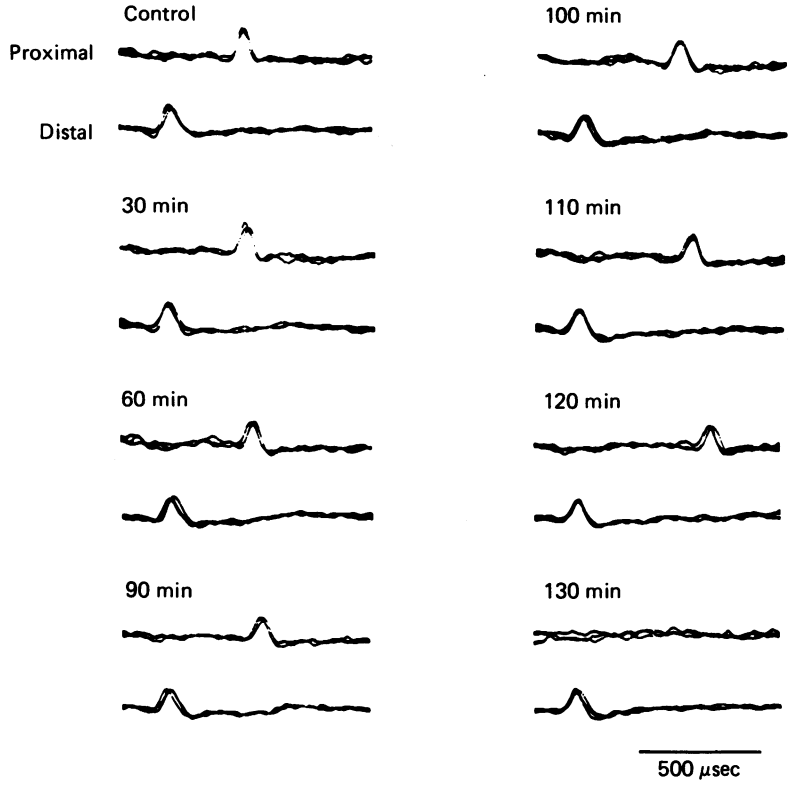

Fig. 3. Responses in a single fibre at recording sites 11·5 mm apart proximal and distal to the site of AGS application at intervals following serum exposure. The fibre illustrated is the fourth of the five fibres illustrated in Fig. 1.

Fig. 5 illustrates the interval between serum application and conduction block for thirty-one fibres from five roots of five animals exposed to two different antisera. This graph represents only fibres in which conduction block occurred within the first 5 hr of exposure to the serum. The minimum time of exposure to serum preceding conduction block was as little as 1 hr for small diameter fibres with conduction velocity 20–30 m/sec but was at least 3 hr for the larger diameter fibres with conduction velocity 50–60 m/sec. The access of the serum to individual nerve fibres is likely to be influenced by their locations within the root, superficial fibres being more immediately exposed than those further from the surface. None the less Fig. 5

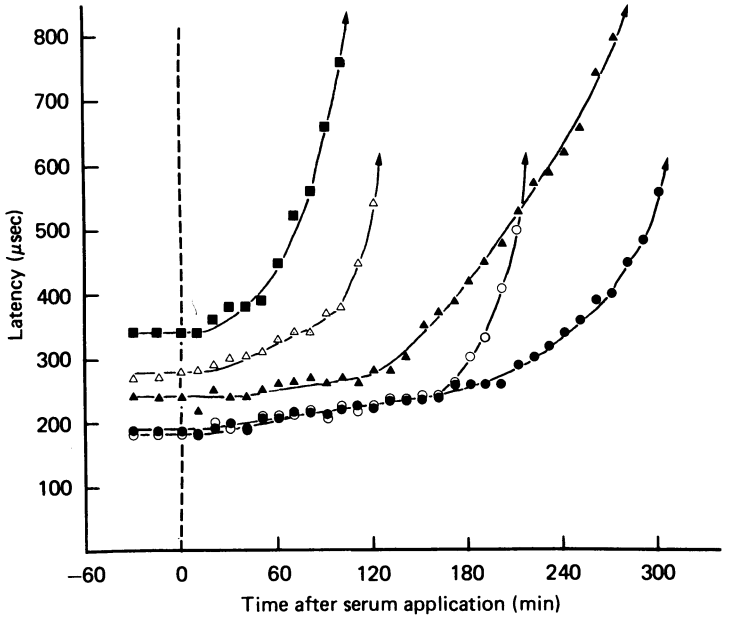

Fig. 4. Conduction times for the five single fibres illustrated in Fig. 1 over 11·5 mm of ventral root before, and after application of AGS. For each unit conduction block is indicated with an arrow.

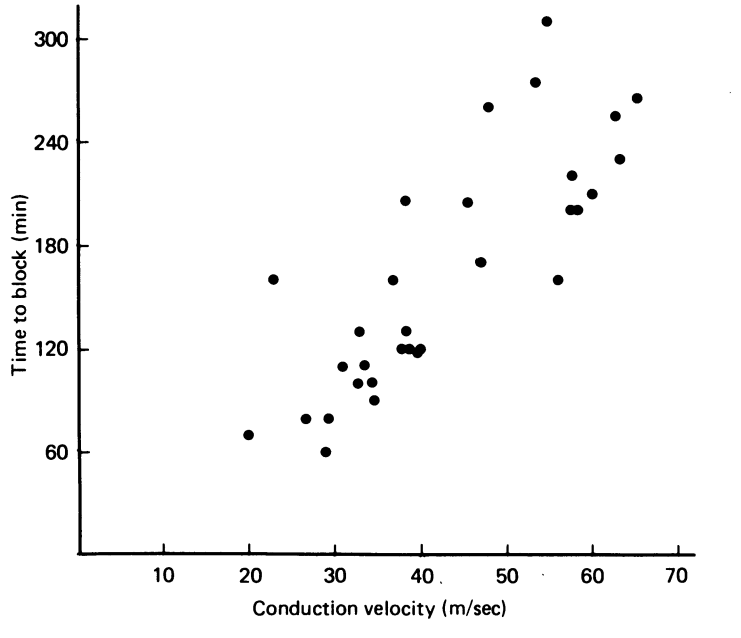

Fig. 5. Interval between AGS application and conduction block as a function of conduction velocity before AGS application.

illustrates an impressive differential susceptibility among affected fibres, the more slowly conducting myelinated axons in general sustaining conduction block earlier than more rapidly conducting myelinated axons.

Extensive control experiments demonstrating that non-immunized and antibody-depleted sera have no blocking effect have previously been performed using the rat

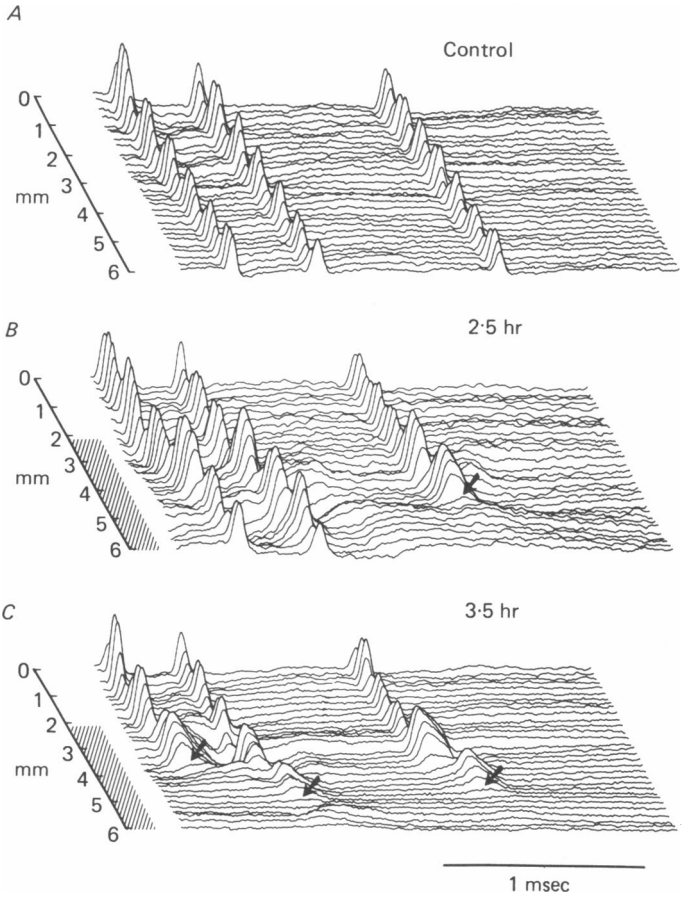

Fig. 6. External longitudinal current recordings for three fibres at intervals of 200 μm over 6 mm of ventral root. Direction of propagation from above downwards. *A*, before AGS application; *B*, 2·5 hr after exposure to AGS of the portion of the root indicated by cross-hatching; *C*, 3·5 hr after AGS exposure. There was no current calibration for these records. The decreased amplitude of the latter records in *C* probably reflects some shunting between the recording electrodes.

sciatic nerve preparation (Sumner *et al.* 1981) and such controls were not repeated in this series of experiments. However several experiments were done using sera inadvertently stored at −20 °C for 4 months. In these experiments conduction block was infrequent and only observed after 10–12 hr exposure to the serum. Sera from the same animals stored for many more months at −70 to −90 °C retained normal blocking activity. The experiments with the sera stored at −20 °C served as a useful

control to demonstrate the stability of conduction time of single units for as long as 12 hr in this preparation when exposed to inactive sera.

Changes in internodal conduction time following exposure to AGS

In order to observe directly the conduction of impulses within the affected area, the well and its contained serum were removed after the root had been bathed in serum for about 2 hr. Repeated external longitudinal current recordings were then made at intervals of 200 μm on either side of and within the site of exposure to the serum as illustrated in Fig. 6. The positions of nodes of Ranvier can be inferred from the

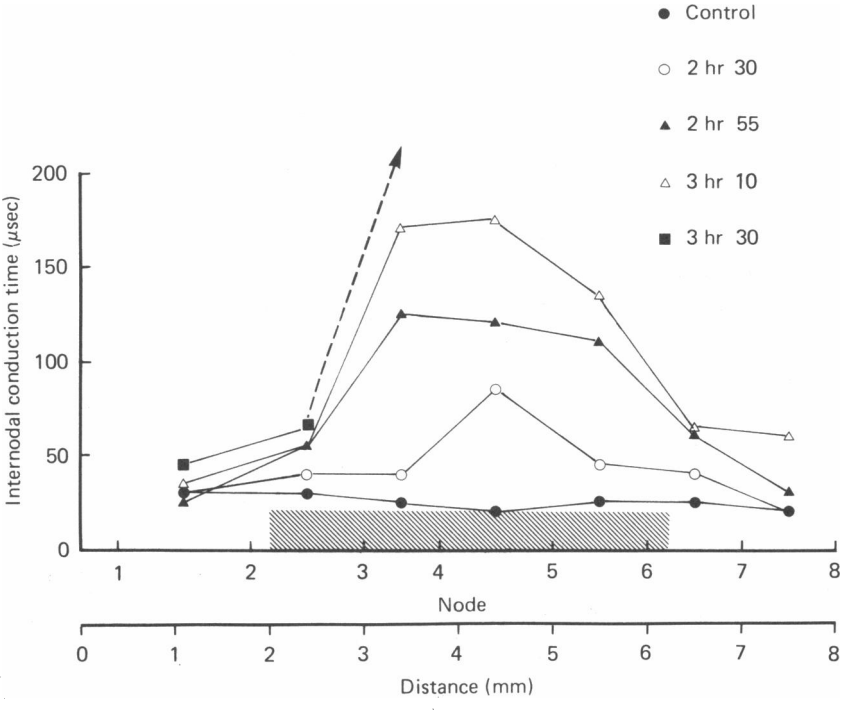

Fig. 7. Internodal conduction time across seven successive internodes of a ventral root fibre before and at intervals following exposure to AGS over the portion of the fibre indicated by cross-hatching.

positions of the periodic maxima of external longitudinal current (Rasminsky & Sears, 1972; Bostock & Sears, 1978). The inferred positions of the nodes remained constant through several hours of repeated scanning of the root with the mobile electrodes.

For the first of the three fibres displayed in Fig. 6*A* there is a local maximum of amplitude at the second recording site from the top of the figure and five subsequent maxima defining five internodes with average internodal length of 1·08 mm. The successive records for the second and third fibres define six internodes over the displayed recording stretch of 6 mm for each of these fibres. After 2·5 hr exposure to the serum (Fig. 6*B*), conduction block occurred at the sixth node of the third fibre (arrow) in the centre of the area of serum application; after a further hour's exposure

(Fig. 6*C*), conduction block had also occurred in the first and second fibres (arrows) at nodes within a mm of the site of blockage in the third fibre.

Fig. 7 illustrates the progressive increase in internodal conduction time within the region of serum exposure for one of these fibres. Internodal conduction time characteristically increased as in this example from control values of 20–25 μsec to about 200 μsec just before conduction block. Immediately prior to conduction block, conduction became intermittent with substantial jitter and was dependent on both frequency (Rasminsky & Sears, 1972) and temperature (Rasminsky, 1973). The intermittency of conduction is not demonstrated in the computer averaged records but could be seen on observation of single sweeps on the oscilloscope.

Simultaneous measurement of membrane current and extracellular potential

In order to determine the mechanism of conduction block we compared the conduction block caused by AGS to that caused by agents preventing excitation of axon membrane.

Tetrodotoxin and local anaesthetic. Fig. 8 illustrates simultaneous recordings of membrane current and extracellular potential from a single fibre within a root focally exposed over a length of 3–4 mm to a drop of tetrodotoxin (TTX) $1{\cdot}5 \times 10^{-6}$ M. Conduction block occurred immediately after the TTX was applied and persisted after the drop was gently sucked away from the root. In Fig. 8 the sites of the last three active nodes N1–N3 are identified as sites of inward membrane current flow and the site of node N4 is identified as a focal site of increased passive outward current flow. The displacement of extracellular potential at node N4, the site of propagation failure, is 45 % of the displacement of potential seen in the non-anaesthetized portion of the fibre. This reflects a displacement of nodal membrane potential of about 45 mV, clearly well above threshold for a non-anaesthetized node. Similar results were obtained from fibres exposed to lignocaine 0·1 %. In those cases where the preceding nodes were partially anaesthetized, the displacement of potential at the first blocked node was less than that shown in Fig. 8.

AGS. Fig. 9*A* shows typical membrane current and extracellular potential records made over several internodes approaching the site of conduction block in a fibre exposed to AGS for 2½ hr. The four active nodes N1–N4 are identified as the sites of generation of inward membrane current. The first inactive node N5 is identified as the site of large outward current flow coincident in time with the inward current generated at node N4. The potential displacement in the potential recordings at the blocked node is only 8 % of that in the normal portions of the fibre, clearly insufficient to cause a regenerated action potential at this node. The displacement of membrane potential at the last active node N4 just before it reaches threshold is reflected by the potential at the inflexion point of the potential records on either side of this node, i.e. 15–20 % of the potential displacement in the normal portion of the fibre corresponding to a membrane potential displacement of close to 20 mV. Fig. 9*B* shows membrane current and potential recordings from the same fibre 3 hr later when the site of conduction block had moved back from node N5 to node N4. Node N4 now fails to be depolarized to threshold and there is virtually no displacement of membrane potential at node N5.

The difference between conduction block caused by AGS and that caused by TTX

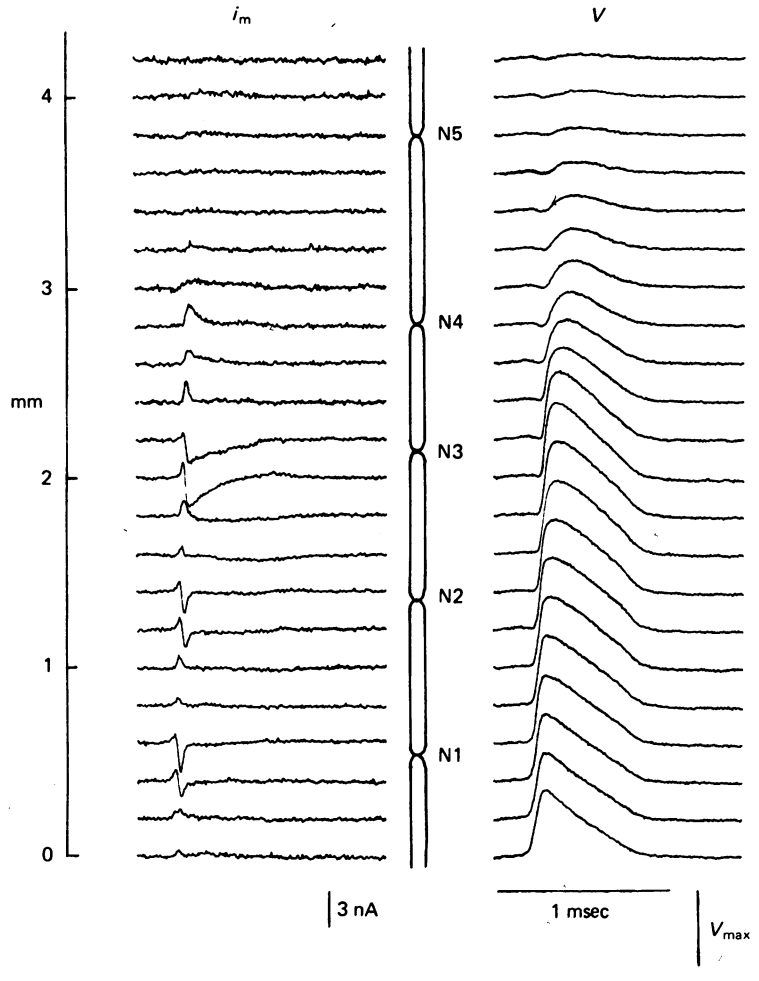

Fig. 8. Membrane current (i_m) and extracellular potential (V) at successive sites along a ventral root fibre focally exposed to TTX, $1{\cdot}5 \times 10^{-6}$ M. The direction of propagation is upward and the positions of the nodes of Ranvier N1–N4 are inferred from the derived membrane current records. In this and the subsequent Figures upward and downward deflexions reflect outward and inward membrane current respectively. The potential calibration in this and the subsequent Figures is the full action potential V_{max} recorded in the portion of the root in which conduction is normal.

or local anaesthetic is clearly seen by comparing the membrane currents and potentials at the nodes where conduction block occurs. Several such nodes are illustrated in Fig. 10. At nodes where conduction is blocked by TTX or local anaesthetic, a relatively small outward current is associated with a relatively large displacement of membrane potential. In contrast, at nodes where conduction is blocked by AGS, a relatively large outward current is associated with a relatively small displacement of membrane potential. This must reflect an increased capacitance and decreased resistance of the nodes exposed to the AGS.

Estimation of nodal capacitance and resistance

The eqns. 3–6 (see Methods) can be solved for c_n and r_n providing that r_n is not voltage- or time-dependent. We have assumed this condition to be fulfilled at nodes anaesthetized by lignocaine or tetrodotoxin or at nodes which fail to be depolarized to threshold for excitation following serum exposure.

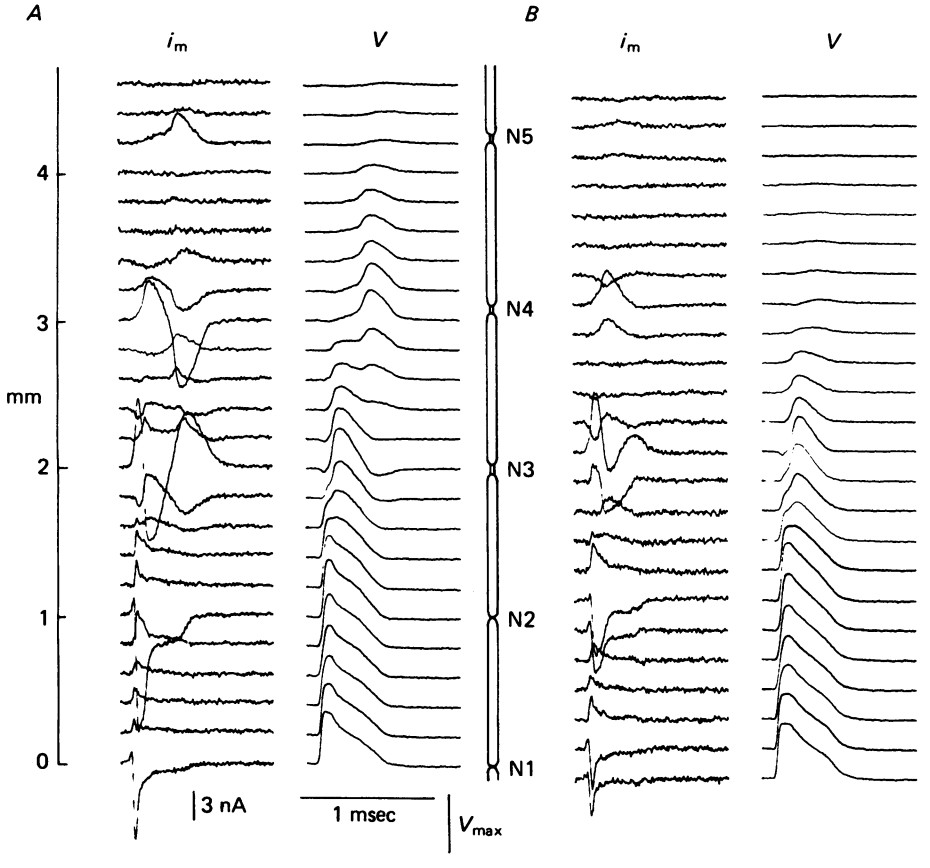

Fig. 9. Membrane current (i_m) and extracellular potential (V) at successive sites along a ventral root fibre focally exposed to AGS for A, $2\frac{1}{2}$ and B, $5\frac{1}{2}$ hr. The direction of propagation is upward and the positions of the nodes of Ranvier N1–N5 are inferred from the derived membrane current records.

For these computations passive nodes were identified as focal sites of increased outward current flow at appropriate positions on the fibre as defined by the internodal distance between more distal active nodes. It was important to be assured that the membrane current records used for the computations reflected all of the current flowing through the nodes. This would only be the case if the two successive external longitudinal current recordings used to derive the membrane current were taken from either side of the node, as for example at node N5 in Fig. 9*A*, where a large outward

membrane current is seen at only one site. However, if an external longitudinal current recording site straddles a node, the difference between the recording from this site and each of its neighbouring sites will reflect only a portion of the nodal current, as for example at node N4 of Fig. 9*B*, where substantial outward current is seen at two adjacent sites. This situation would lead to an underestimate of nodal current.

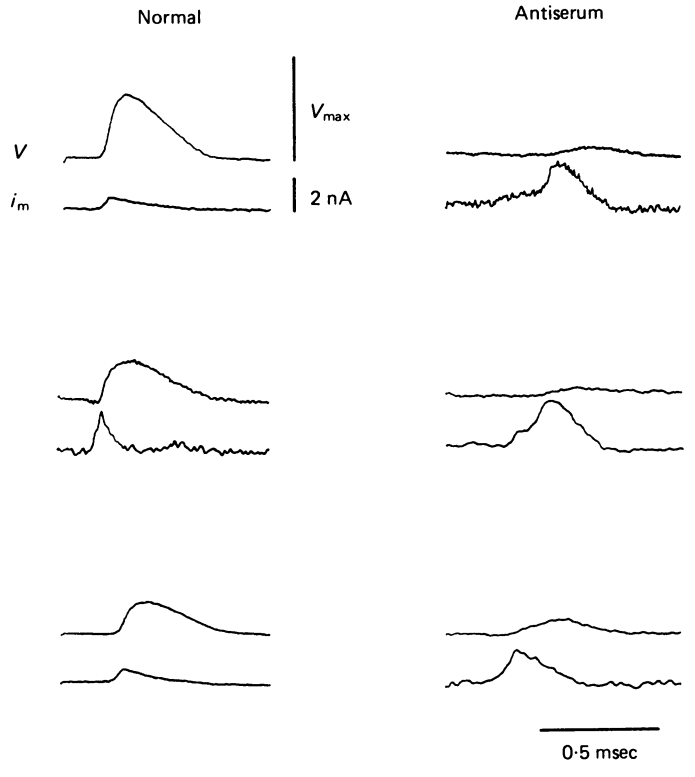

Fig. 10. Membrane current and extracellular potential at nodes where conduction failure is due to TTX or local anaesthetic (left) or to exposure to AGS (right). Current, voltage and time scales are the same for all pairs of records.

For this reason, the membrane currents used for the computations of c_n and r_n were all derived by differencing external longitudinal current records two recordings sites (400 μm) apart, omitting the intervening record closest to or straddling the node. The membrane currents derived in this way reflect both nodal and extranodal current and thus give rise to an over-estimate of nodal capacitance and an underestimate of nodal resistance. The potential records used for the computations were those judged to be closest to the node, i.e. those corresponding to the largest outward current obtained by differencing adjacent external longitudinal current records in the vicinity of the nodes.

Fig. 11*A* shows an example of the close fit between the potential displacement predicted by eqn. (4) and the recorded potential displacement at a normal node inactivated by local anaesthetic. For this node the calculated capacitance and

resistance were 1·2 pF and 71 MΩ. The average nodal capacitance was 2·6 ± 0·3 (S.E.) pF, average nodal resistance 55 ± 10 MΩ and average time constant 143 ± 38 μsec for thirteen anaesthetized or TTX-inactivated nodes from twelve fibres of internodal lengths 0·8–1·1 mm.

The data for serum exposed nodes at which conduction failed is summarized in Table 1. The calculated values for nodal capacitance varied greatly, ranging from 12

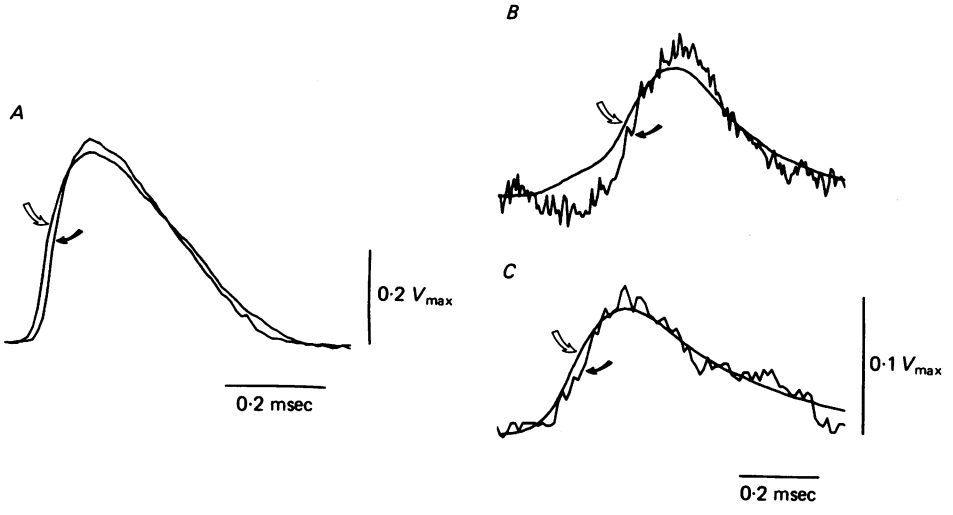

Fig. 11. Recorded (dark arrows) and fitted (open arrows) potential displacements, *A*, at a locally anaesthetized node and *B* and *C*, at nodes exposed to AGS. Time and voltage scale same for *B* and *C*.

to 56 pF. The corresponding values for nodal resistance ranged from 5 to 22 MΩ, the average membrane time constant of 271 ± 25 μsec being significantly greater for serum-treated than normal nodes. Fig. 11*B* and *C* shows examples of the fit between the potential displacement predicted by eqn. (4) and the recorded potential displacement at nodes where conduction is blocked following exposure to AGS.

The estimates of nodal capacitance and resistance were subject to a number of errors due to inaccuracies in measurement and calibration of membrane current and potential and to artifacts inherent in the recording techniques. The major of these are enumerated below.

(1) The computations of c_n and r_n assume that the recorded potential changes are proportional to transmembrane potential and that the normal action potential is 100 mV. The major justification for the former assumption is that the externally recorded potential displacement remains relatively constant over several mm in normal fibres. Although the amplitude of the normal myelinated fibre action potential may differ somewhat from the assumed 100 mV, any difference would have a similar effect on the computations for both the anaesthetized and serum-exposed nodes and would have no effect on the proportional changes computed in c_n and r_n.

(2) In many potential records, particularly in the vicinity of nodes of Ranvier, there is an early phase of apparent hyperpolarization that is almost certainly a volume conductor recording artifact reflecting eccentric circuitous paths of current flow extracellular to active fibres within the ventral root (Bostock & Sears, 1978). This early apparent hyperpolarization was variable from fibre to fibre but was in general much more striking near serum-exposed nodes than near anaesthetized nodes. Such early apparent hyperpolarization is apparent at nodes N3 and N4 of the fibre illustrated in Fig. 9*A* and accounts for most of the discrepancy between the observed and fitted potential

displacement at the serum exposed node illustrated in Fig. 11*B*. The amplitude of the fitted potential is in fact somewhat less than that of the recorded potential as a consequence of the procedure for minimizing the mean-square error between the experimental data and model output which is performed over the entire time domain of the action potential. The true transmembrane potential is thus probably similar in shape but somewhat greater in amplitude than the fitted potential; for this reason our calculated values for the resistance of nodes where the apparent hyperpolarizing artifact is present are almost surely underestimates, and the calculated values for capacitance over-estimates. The larger values for capacitance were in fact computed for nodes at which the apparent hyperpolarizing artifact was most prominent.

TABLE 1. Nodal capacitance and nodal resistance of normal and serum-exposed nodes

	Nodal capacitance (pF)	Nodal resistance (MΩ)	Nodal time constant (μsec)
Normal nodes ($n = 13$)	2·6 ± 0·3	55 ± 10	143 ± 38
Serum-exposed nodes	39	5·4	
	56	5·6	
	16	22	
	12	16	
	16	22	271 ± 25*
	34	11	
	46	5·9	
	21	8·7	

* Significantly greater than normal ($P < 0·05$). All average values ± S.E. of means.

(3) There is some uncertainty concerning the absolute values of the membrane currents since, as pointed out by Bostock & Sears (1978), the extracellular pathways of current flow are not necessarily identical for the action currents and calibration currents.

As noted above, a more substantial difficulty may arise because the membrane current records reflected not only nodal but also extranodal membrane current. The ratio of extranodal to nodal capacitance would be expected to be greater for the normal fibres than for those exposed to AGS. We thus think it likely that nodal capacitance is proportionately more over-estimated for the normal nodes than for those exposed to antiserum. Using membrane current records derived from adjacent external longitudinal current records (i.e. 200 μm apart), the average normal nodal capacitance was recalculated as 1·5 ± 0·2 pF. This is almost surely an underestimate since many of the membrane current records used for these computations were derived from pairs of external longitudinal current records in which one record straddled the node. We thus think it likely that the true value for average nodal capacitance lies between the extremes of 1·5 ± 0·2 pF and 2·6 ± 0·3 pF.

(4) The values obtained for nodal resistance were much more scattered than those for nodal capacitance. The reason for this is apparent on consideration of eqns. (7) and (8) (see Methods) which are used to calculate capacitance and resistance. It was always the case that $1 > a_0 > 0·9$ and thus small errors in estimation of a_0 would result in large errors in estimation of

$$r_n = \frac{b_0}{1-a_0}.$$

The expression for

$$c_n = \frac{-T_s(1-a_0)}{b_0 \ln a_0}, \tag{8}$$

can be rewritten using the Taylor expansion of $\ln a_0$ to give

$$c_n = \frac{-T_s(1-a_0)}{b_0\left[(a_0-1)-\frac{(a_0-1)^2}{2}+\frac{(a_0-1)^3}{3}-\frac{(a_0-1)^4}{4}+\ldots\right]}. \tag{9}$$

For $1 > a_0 > 0{\cdot}9$, the expansion of $\ln a_0$ is dominated by the first term and eqn. (9) reduces to

$$c_n \approx \frac{T_s}{b_0}. \tag{10}$$

The computed value of c_n is thus extremely insensitive to errors in estimation of a_0. For this reason we regard values obtained for nodal capacitance from the normal fibres as much more reliable than those for nodal resistance or membrane time constant.

Despite the uncertainties outlined above in the measurement of absolute values of nodal capacitance and resistance, it is clear that there is about an order of magnitude increase in the capacitance of serum exposed nodes at the sites of conduction failure and a fall in resistance that may be somewhat less.

Late outward current at serum-exposed nodes

At some nodes such as node N3 of Fig. 9*A* a large late phase of outward membrane current followed the initial phase of inward membrane current. At least some of this outward membrane current originated as inward membrane current at node N4 and, as can be seen in Fig. 9*B*, was substantially reduced but not abolished when excitation failed at node N4. It is likely that at least some of this late outward current is potassium current as has been described at chronically demyelinated mammalian nodes (Sherratt, Bostock & Sears, 1980) and at osmotically disrupted mammalian nodes (Chiu & Ritchie, 1980, 1981). Although several nodes generating late outward current were seen in our experiments, this was not an invariable concomitant of acutely increased nodal capacitance; for example there is no suggestion of a late outward nodal current in the nodes N4 and N2 adjacent to node N3.

Mammalian nodal axon membranes appear to be normally devoid of potassium channels (Horáckova, Nonner & Stämpfli, 1968; Bostock, Sherratt & Sears, 1978; Brismar, 1980; Chiu, Ritchie, Rogart & Stagg, 1979), and Chiu & Ritchie (1981) have speculated that a function of paranodal potassium channels may be to prevent re-entry excitation and reflexion of impulses at demyelinated nodes by clamping the membrane potential near the resting potential. Node N3 in Fig. 9*A* may represent an example of this phenomenon. Although the node is stimulated during the late falling phase of the action potential with a large outward membrane current originating at node N4, re-excitation of the node does not occur. In fact there appears to be a late phase of hyperpolarization at this node which could reflect increased potassium conductance.

DISCUSSION

In these experiments we have observed at a single-fibre level the changes in propagation of nerve impulses which occur during acute antibody-mediated demyelination. Following exposure of normal nerve fibres to AGS, nerve impulses are transmitted with progressively increased conduction time across internodes exposed to the antiserum. Conduction ultimately fails at an exposed node when the propagating impulse fails to depolarize the nodal axon membrane to threshold. This mechanism of conduction failure is in striking contrast to that observed at anaesthetized nodes at which regeneration of the nerve impulse can fail to occur despite depolarization of the nodal membrane well beyond the normal threshold potential. The conduction

changes caused by the AGS thus cannot be primarily due to changes in the voltage-sensitive permeability properties of nodal axon membrane but must rather be due primarily to changes in the cable properties of the fibres.

The morphological changes observed in rat spinal root fibres during the first few hours of exposure to AGS include alterations in Schmidt–Lanterman clefts and disruption of myelin in the paranodal region, with detachment of the outermost paranodal myelin loops from paranodal axon and a consequent increase in nodal surface area (Brown, Sumner, Saida & Asbury, 1980). We believe the latter change to be most critical from a physiological point of view as it would satisfactorily account for the observed increased in nodal capacitance and fall in nodal resistance. Computer simulations (Koles & Rasminsky, 1972) suggest that although an initial small increase in nodal or internodal capacitance and conductance would have relatively little effect on internodal conduction time, further similar increases in capacitance and conductance would cause progressively greater increases of internodal conduction time prior to conduction block. The initially slow and subsequent rapid increase in conduction time through the portion of fibres exposed to AGS could reflect a relatively uniformly progressive increase in nodal surface area with time of exposure to the antiserum.

If resistivity and capacitivity were the same for paranodal and nodal axon membrane, any increase in nodal capacitance would be associated with an equivalent fall in nodal resistance, and the membrane time constant would remain unchanged. In fact the fall in resistance was in general less than the increase in capacitance, suggesting that the resistivity of the newly exposed paranodal axon membrane is greater than that of the nodal axon membrane. The same discrepancy between the increase in nodal capacitance and fall in nodal resistance was observed by Chiu & Ritchie (1980, 1981) during acute demyelination with osmotic shock or lysolecithin.

It is likely that the critical effect of the AGS is to disrupt the axoglial junction in a spiral fashion beginning at the outermost paranodal loops to which the serum has initial access. This postulated mechanism of action may provide an explanation for the differential susceptibility of small fibres. The internodal capacitance and conductance of small fibres is less than that of larger fibres. Even though the rate of increase of nodal area following serum exposure might be similar for small and large fibres, it is likely that the increase in the *ratio* of nodal to internodal capacitance and conductance would be much more precipitous in the smaller fibres, thus giving rise to more rapid change in conduction properties.

Differences in morphology of nodes of small and large fibres (Berthold, 1978) may be another important factor in their apparent differential susceptibility to the effects of the antiserum. In large fibres access of AGS to the region of axoglial apposition may be more restricted than in small fibres because of the Schwann cell microvilli within the extranodal region. Brown *et al.* (1980) have in fact observed that pathological changes appear to occur more rapidly in the small diameter axons on exposure to AGS.

Whatever the explanation for the observed differential susceptibility of smaller fibres, the phenomenon clearly elucidates the earlier observations of Sumner *et al.* (1981) on the effects of intraneural injection of AGS into rat sciatic nerves. In these experiments the muscle compound action potential elicited by simulation of the

sciatic nerve above the injection site fell in amplitude, with very little change in latency over the first 2–4 hr following injection. It now seems clear that the fall in amplitude reflected preferential blockage of the more slowly conducting fibres, while the unchanging latency reflected the delay in significant change in conduction velocity of the larger fibres.

The question arises as to the importance of the changes observed in the Schmidt–Lanterman clefts on exposure to AGS. Measurements of the resistance and capacitance of normal internodal myelin are unreliable using our technique because of the low signal-to-noise ratio for membrane current measurements in mid-internode. It was thus impossible to assess precisely the extent of the change in internodal resistance and capacitance secondary to serum exposure. It was however the case that internodal current leakage was invariably very much less than that at the nodes for the serum exposed fibres. We thus believe that any increased leakage through the dilated Schmidt–Lanterman clefts was of relatively minor importance in relation to the changes in current flow caused by the increase in nodal capacitance and fall in nodal resistance.

Other changes which could cause conduction slowing and block include a decrease in nodal resistivity due to a direct effect of AGS on nodal axon membrane and/or depression of the regenerative properties of axon membrane. As noted above, the resistance of the node does not fall in proportion to the increase in capacitance; it is thus very unlikely that AGS has any direct effect on the resistivity of the nodal axon membrane. Our experiments do not definitively exclude the possibility of a minor effect on the regenerative properties of axon membrane. It is unlikely that this is a major factor since regeneration of the action potential invariably occurred at serum-exposed nodes if their membrane potential was displaced from resting potential to a threshold of less than 20% of the normal action potential amplitude (as at node N4 of the fibre illustrated in Fig. 9*A*).

Previous studies of the propagation of impulses in single demyelinated nerve fibres have all been performed several days after exposure to a demyelinating agent such as diphtheria toxin (Rasminsky & Sears, 1972; Bostock & Sears, 1976, 1978) or lysolecithin (Bostock, 1981; Bostock, Hall & Smith, 1981). The non-uniformity of the pathological lesion in these relatively chronic preparations has precluded identification of the minimal lesion required for conduction block since it has been, as yet, impossible to study the same pathological axon both physiologically and morphologically. The present experiments suggest that, at least in the acute situation, a modest degree of paranodal demyelination is sufficient for conduction block. Because of the plasticity of axon membrane properties, paranodal demyelination may be of much less physiological significance in the more chronic situation after new sodium channels have been inserted into the previously inexcitable paranodal axon membrane. Bostock & Sears (1978) provide some experimental evidence that the increase in nodal capacitance of diphtheria demyelinated nodes may be compensated by an increase in sodium channel density, and Moore, Joyner, Brill, Waxman & Najar-Joa (1978) have shown that in computer-simulated myelinated axons, conduction velocity is relatively insensitive to nodal area provided that the density of sodium channels per unit area is constant. Chiu & Ritchie (1980, 1981) note that total nodal sodium current does not increase with the increase in nodal capacitance during

osmotic or lysolecithin-mediated disruption of mammalian nodes of Ranvier in a voltage clamp. In acute paranodal demyelination it is thus likely that the average density of sodium channels in the exposed axon membrane in the vicinity of the node falls as paranodal demyelination ensues, even though the total number of sodium channels per node may remain constant.

The measured capacitances of nodes at which conduction block occurred were highly variable and we can offer no figure for the smallest increase in nodal capacitance required to cause conduction block. This is hardly surprising; the amount of nodal disruption tolerated by a given node will be at least to some extent a function of the severity of the pathology of the adjacent node(s). Computer simulations (Koles & Rasminsky, 1972) have shown that a severity of demyelination consistent with propagation across a single internode leads to conduction block if imposed on two adjacent internodes.

The experiments reported in this paper have examined only the very acute effects of exposure to AGS. The more long-term consequences of antiserum-induced focal demyelination have been examined serially following intraneural injection of rat sciatic nerve (Saida *et al.* 1980; Sumner *et al.* 1981). In this preparation there is a similar acute onset of conduction block which then persists unchanged for 5–8 days concomitant with the evolution of the morphological lesion from paranodal to segmental demyelination. Recovery of conduction beginning at 7–9 days is associated with early remyelination.

These experiments suggest that the rapid development of symptoms characteristic of acute demyelinating neuropathies could be caused by the earliest changes of paranodal demyelination. Antibodies to galactocerebroside or other components of myelin could be of pathogenic importance in disorders such as the Guillain–Barré syndrome due to physiological effects of the type which we have reported in this paper.

The work was supported by grants from the Canadian Medical Research Council and the U.S. National Institutes of Health (grant no. NS 08075).

REFERENCES

BERTHOLD, C.-H. (1978). Morphology of normal peripheral axons. In *Physiology and Pathobiology of Axons*, ed. WAXMAN, S. G., pp. 3–63. New York: Raven Press.

BOSTOCK, H. (1981). Conduction changes in demyelination. In *Abnormal Nerves and Muscles as Impulse Generators*, ed. CULP, W. & OCHOA, J. New York: Oxford University Press (in the Press).

BOSTOCK, H., HALL, S. M. & SMITH, K. H. (1981). Demyelinated axons form 'nodes' prior to remyelination. *J. Physiol.* **308**, 21–22*P*.

BOSTOCK, H., SHERRATT, R. M. & SEARS, T. A. (1978). Overcoming conduction failure in demyelinated nerve fibres by prolonging action potentials. *Nature, Lond.* **274**, 385–387.

BOSTOCK, H. & SEARS, T. A. (1976). Continuous conduction in demyelinated mammalian nerve fibres. *Nature, Lond.* **263**, 786–787.

BOSTOCK, H. & SEARS, T. A. (1978). The internodal axon membrane: electrical excitability and continuous conduction in segmental demyelination. *J. Physiol.* **280**, 273–301.

BRISMAR, T. (1980). Potential clamp analysis of membrane currents in rat myelinated nerve fibres. *J. Physiol.* **298**, 171–184.

BROWN, M. J., SUMNER, A. J., SAIDA, T. & ASBURY, A. K. (1980). The evolution of early demyelination following topical application of anti-galactocerebroside serum *in vivo*. *Neurology, Minneap.* **30**, 371.

CHIU, S. Y. & RITCHIE, J. M. (1980). Potassium channels in nodal and internodal axonal membrane of mammalian myelinated fibres. *Nature, Lond.* **284**, 170–171.

CHIU, S. Y. & RITCHIE, J. M. (1981). Evidence for the presence of potassium channels in the paranodal region of acutely demyelinated mammalian single fibres. *J. Physiol.* **313**, 415–437.

CHIU, S. Y., RITCHIE, J. M., ROGART, R. B. & STAGG, D. (1979). A quantitative description of membrane currents in rabbit myelinated nerve. *J. Physiol.* **292**, 149–166.

HORÁCKOVA, M., NONNER, W. & STÄMPFLI, R. (1968). Action potentials and voltage clamp currents of single rat Ranvier nodes. *Proc. int. Union physiol. Sci.* XXIV, **7**, 198.

KATZ, B. (1966). *Nerve, Muscle and Synapse.* New York: McGraw-Hill.

KOLES, Z. J. & RASMINSKY, M. (1972). A computer simulation of conduction in demyelinated nerve fibres. *J. Physiol.* **227**, 351–364.

MOORE, J. W., JOYNER, R. W., BRILL, M. H., WAXMAN, S. G. & NAJAR-JOA, M. (1978). Simulations of conduction in uniform myelinated fibres: relative sensitivity to changes in nodal and internodal parameters. *Biophys. J.* **21**, 147–160.

RASMINSKY, M. (1973). The effects of temperature on conduction in demyelinated single nerve fibers. *Archs Neurol., Chicago* **28**, 287–292.

RASMINSKY, M. & SEARS, T. A. (1972). Internodal conduction in undissected demyelinated nerve fibres. *J. Physiol.* **227**, 323–350.

ROSENBROCK, H. H. (1966). *Computational Techniques for Chemical Engineers.* London: Pergamon Press.

SAIDA, K., SAIDA, T., BROWN, M. J. & SILBERBERG, D. H. (1979) *In vivo* demyelination induced by intraneural injection of anti-galactocerebroside serum. *Am. J. Path.* **95**, 99–116.

SAIDA, K., SUMNER, A. J., SAIDA, T., BROWN, M. J. & SILBERBERG, D. H. (1980). Antiserum-mediated demyelination: relationship between remyelination and functional recovery. *Ann. Neurol.* **8**, 12–24.

SHERRATT, R. M., BOSTOCK, H. & SEARS, T. A. (1980). Effects of 4-aminopyridine on normal and demyelinated mammalian nerve fibres. *Nature, Lond.* **283**, 570–572.

SMITH, J. M. (1977). *Mathematical Modelling and Digital Simulations for Engineers and Scientists.* New York: John Wiley & Sons.

SUMNER, A. J. (1981). The physiological basis of symptoms in Guillain–Barré syndrome. *Ann. Neurol.* **9** (suppl.), 28–30.

SUMNER, A. J., SAIDA, K., SAIDA, T., SILBERBERG, D. H. & ASHBURY, A. K. (1981). Acute conduction block associated with an antiserum-induced demyelinative lesion of peripheral nerve. *Ann. Neurol.* (in the Press).